

## Generation of low-temperature plasma by low-pressure arcs for synthesis of nitride coatings

O V Krygina<sup>1,2</sup>, N N Koval<sup>1,2</sup>, I V Lopatin<sup>1</sup>, V V Shugurov<sup>1</sup>, and S S Kovalsky<sup>1,2</sup>

<sup>1</sup>Institute of High Current Electronics SB RAS, Tomsk, 634055, Russia

<sup>2</sup>National Research Tomsk State University, Tomsk, 634050, Russia

E-mail: [krygina\\_82@mail.ru](mailto:krygina_82@mail.ru)

**Abstract.** Experiments were performed to study gas, metal, and mixed metal-gas plasmas. The plasmas were generated with the use of an arc evaporator and a gas-plasma source with a hot filament and hollow cathode that were operated independently or simultaneously. It has been revealed that the arc current of gas-plasma source affects the parameters of the metal-gas plasma and the element concentrations in the coatings. It has been demonstrated that the characteristics of the nitride coatings produced by plasma-assisted vacuum-arc deposition can be controlled by varying the parameters of the arc in the gas-plasma source.

### 1. Introduction

Physical vapor deposition (PVD) of protective coatings on the surfaces of machine parts, tools, and products is a widely used technique to increase their service life and extend their field of use due to the unique properties of the coatings. In particular, high performance coatings are produced using the well-known binary titanium nitride system that is deposited on cutting tools to form wear-resistant high hardness ( $H = 20\text{--}25$  GPa) coatings or on various products to form golden decorative coatings.

The vacuum-arc coating deposition technique based on condensation of the plasma generated by a low-pressure arc with a cathode spot [1] shows versatility, high deposition rate ( $\sim 10$   $\mu\text{m/h}$ ), and other advantages, thus being among the most efficient methods of plasma-ion synthesis of functional coatings.

Usually, the nitrogen pressure, discharge current, substrate temperature, bias voltage are the varied parameters by optimization of nitride coatings deposition modes [2–7]. On the other hand, the authors of a great number of publications on plasma-ion deposition of functional coatings point to the use of additional devices (ion or electron sources, plasma filters, etc.) [8–10], or complex compositions of vaporized targets, or working gas mixtures, etc. This makes every work original and enables one to vary the structure and properties of coatings over wide limits. In our case, the coatings were synthesized by the plasma-assisted vacuum-arc deposition technique using the hot filament, hollow cathode plasma generator [11, 12] developed at the Institute of High Current Electronics, SB RAS (Tomsk, Russia) and named PINK (Russian acronym) as an accessory plasma source. The PINK generator is well suited to perform cleaning, activation, and heating of various surfaces, plasma-ion etching to remove layers of different thickness, nitriding, and plasma-ion assistance in depositing various-purpose coatings [13–15].

It is well known that the properties, chemical composition, and structure of a coating produced by vacuum-arc deposition and the pattern of plasma chemical reactions taking place on the substrate are substantially determined by the characteristics of plasma in the arc gap. Therefore, to investigate the parameters of the plasma that is condensed to form a coating is of importance. In the experiment under



consideration, plasma-assisted vacuum-arc deposition of coatings was used, and the metal-gas plasma generated by a low-pressure arc was the main object of investigation.

The goal of the experiment was to investigate the generation of gas, metal, and metal-gas plasmas, to measure the plasma parameters, and to elucidate the effect of plasma assistance on the characteristics of the coatings synthesized by the vacuum-arc technique.

## 2. Equipment and procedures

The experiment aimed to study the low-temperature plasmas of low-pressure arcs and the plasma-assisted synthesis of coatings was carried out using automated plasma-ion facility developed at the Institute of High Current Electronics, SB RAS (Tomsk, Russia). A schematic diagram of the experimental apparatus is shown in Fig. 1. Plasma was produced with two plasma sources: a DI-100 arc evaporator [13, 16] operating based on a cathode spot arc and the PINK gas plasma source operating based on a non-self-sustained arc with a hot filament, hollow cathode [11–13]. The plasma parameters were measured using a cylindrical Langmuir probe ( $\varnothing$  0.5 mm;  $l$  = 5 mm) and a unique automated probe system.

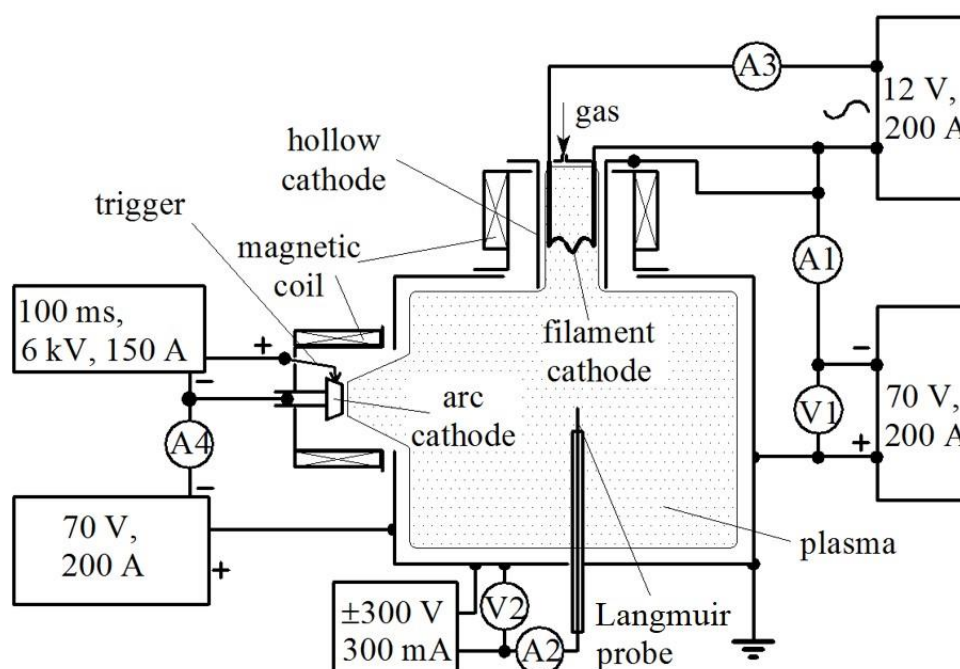


**Figure 1.** Schematic diagram of the experimental apparatus.

A block diagram of the probe measuring system is shown in Fig. 2. Functionally the system can be divided into two units: a measuring unit (MU) and a probe bias unit (PBU). For measuring the probe current-voltage characteristic, a sawtooth voltage or pulse voltage with variable amplitude is applied from the PBU to the probe. To preclude arcing at the probe surface immersed into plasma, the PBU is equipped with additional protective and output-current limiting circuits.

For measuring the probe voltage, a voltage sensor is connected parallel to the probe circuit. For measuring the current, a current sensor is connected in the probe circuit. Signals from both sensors are transmitted through a buffering and amplifying system to a two-channel analogue-to-digital converter (ADC) with a common input for signal conversion. The system provides a minimum phase shift between the current and voltage probe signals.

The system is controlled with a microcontroller, which provides sync signal processing, a delay between the sync signal and startup of the ADC, data transfer from the ADC to a personal computer (PC) through an optical converter, and sync operation of the MU and PBU.

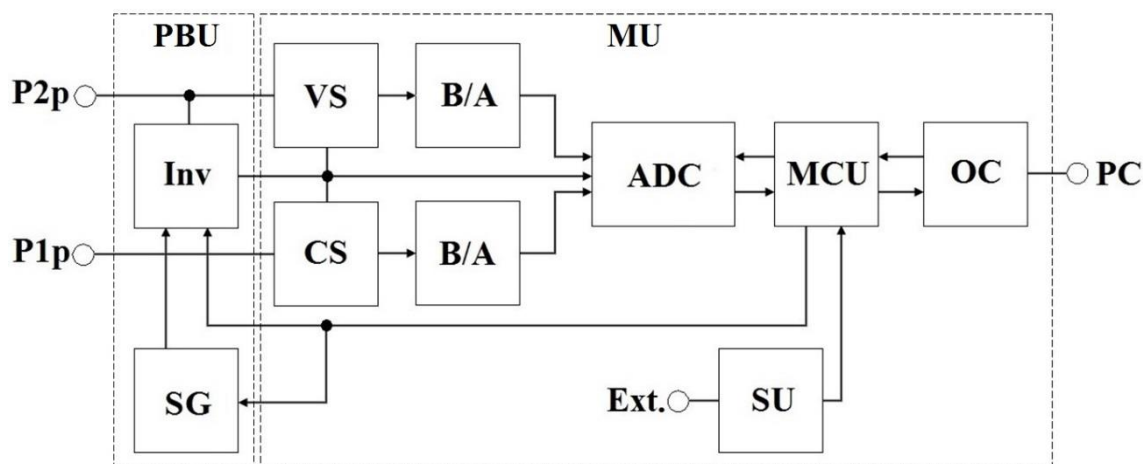


**Figure 2.** Block diagram of the probe measuring system: P1p – connection for a probe; P2p – connection for a reference electrode (or second probe); VS – voltage sensor; CS – current sensor; B/A – buffers and amplifiers; ADC – analog-to-digital converter; Ext – external synchronizer; PC – port for a personal computer; Inv – power inverter; SG – sawtooth voltage generator; PBU – probe bias unit; MU – measurement unit.

The system can be operated in standby and continuous modes. In the continuous mode, each next point of the current-voltage characteristic is recorded as soon as recording of the previous point is completed. If the PBU, in this case, operates in the pulsed mode the bias voltage is applied for the ADC sampling time.

In the standby mode, the system is triggered by a synchronizer signal. Once the signal is produced, the microcontroller starts up the delay timer (from 5  $\mu$ s to 10 ms). Within a prescribed delay time, the ADC is triggered. If the PBU operates in the pulsed mode, the voltage to the probe is applied 5  $\mu$ s before the ADC is triggered. This is required for the transient processes in the probe circuit to be complete before the point of measurement.

When the system is operated in the mode with ion cleaning of the probe surface from contamination and dielectric inclusions, a negative potential ( $-100$  V) with respect to the reference electrode is applied to the probe between measurements. Cleaning of the probe is possible only in the pulsed mode of the PBU.

Measurement data are stored in special PC software for further processing. The software allows adjustment of the automated plasma measuring system and data storage in a format compatible with Excel, Origin, etc.

The system provides the following: a possibility of research with a single probe and double probe; simultaneous measurements of instantaneous voltage and current; input voltages of  $\pm 100$  V; input currents of  $\pm 300$  mA; fast automatic discrete adjustment of amplification with a factor of 1, 2, 5, 10; protection of analogue inputs from overvoltages and short circuit; an ADC capacity of 14 bits; control of the number of points in a measurement interval and measurement time; an optical input; an adjustable delay between the measurement point and sync pulse from 5  $\mu$ s to 10 ms with a step of 1  $\mu$ s; galvanic decoupling between the measuring unit and PC; a possibility of ion cleaning of the probe at intervals between the measurements.

All measurements were performed with the probe placed at the center of the working chamber, immediately at the cross point of the axes of the plasma sources, 450 mm from the output aperture of the PINK source and 300 mm from the output aperture of the arc evaporator. For each operation mode, the probe current-voltage characteristic was measured from which the floating potential ( $\phi_f$ ) and the plasma potential ( $\phi_{pl}$ ) were evaluated by a graphical method. The electron temperature ( $T_e$ ) was

determined from the probe characteristic plotted on a semilogarithmic scale. The plasma density ( $n$ ) was evaluated from the electron branch of the probe characteristic.

The vacuum system of the ion-plasma facility, which incorporates a sliding vane rotary pump and a turbomolecular pump, is capable to evacuate a vacuum chamber to a residual pressure of  $\sim 10^{-3}$  Pa. Inert argon and reactive nitrogen were chosen as working gases. The working gas pressure was  $\sim 0.3$  Pa for all the modes examined. The gas plasma density, controlled by varying the PINK arc current ( $I_p = 0$ –100 A), was a variable parameter in the probe measurements of the parameters of gas and metal-gas plasmas. Investigations of metal and metal-gas plasmas were carried out at the evaporator arc current  $I_d = 50$  and 100 A. Commercially pure titanium (Grade 2 titanium alloy: 99.3%Ti) was used for the cathode material. Molybdenum alloy, 12Cr18Ni10Ti steel, and WC-8%Co hard alloy were used as substrates for X-ray analysis, elemental, and mechanical investigations, correspondingly.

The gas plasma density was a variable parameter. Other parameters of the coating deposition modes were fixed (evaporator arc current with a titanium cathode  $I_d$ , Ti = 100 A, nitrogen pressure  $p_{N_2} = 0.3$  Pa, and substrate was under floating potential  $\phi_{fl}$ ). The substrates were situated at the center of the working chamber like a probe.

It should be noted that the drop fraction is formed at arc deposition of coatings, but in the paper, the influence of gas plasma source on drop fraction was not investigated. That can be found in earlier works [17, 18].

Investigations of the deposited coatings were carried out by micro- and nanoindentation (PMT-3, NHT-S-AX-000X Nano Hardness Tester). The phase composition was investigated by X-ray diffraction analysis (Shimadzu XRD 6000 X-ray diffractometer). The element concentrations in the TiN coatings were measured by the Auger spectroscopy method. The calculation of nitrogen concentration was carried out by deduction of LMM titanium line intensity from that of overlapped LMM and KLL lines. The intensity of LMM titanium line was calculated from ratio of LMM and LMV titanium lines.

### 3. Results and discussion

In order to reveal how the characteristics of non-self-sustained arc discharge with hot filament and hollow cathode affect the metal-gas plasma parameters the measurements of plasma parameters at (1) independent work of PINK gas-plasma source (gas plasma parameters measurements), at (2) independent work of DI-100 arc evaporator (metal plasma parameters measurements) and at (3) simultaneous work of both plasma sources (metal-gas plasma parameters measurements) were carried out.

#### 3.1. Gas plasma

At first, the gas plasma generated by the PINK plasma source was investigated. The parameters of the argon plasma that was used for pre-cleaning, heating, and activation of the surfaces by plasma-ion etching are presented for different arc operation modes in Fig. 3. An increase in filament current, and, hence, in electron emission current from the filament cathode, increases the PINK arc current and changes the arc operation voltage, leading to an increase in density of the gas plasma.

It has been found that as the arc current was increased from 10 to 90 A, the argon plasma density increased from  $0.3 \cdot 10^{16}$  to  $5.2 \cdot 10^{16} \text{ m}^{-3}$ , resulting in an increase in ion current density at the substrate. Under these conditions, the plasma potential relative to the anode was positive and increased from 5.4 to 6.4 V. The electron temperature  $T_e$  varied inappreciably throughout the current range, and its average value was  $\sim 1.4$  eV.

The measured parameters of the nitrogen plasma that was used for nitriding of extended surface layers of the substrates are given in Fig. 4. The average electron temperature of the nitrogen plasma generated by a low-pressure arc was  $\sim 1.4$  eV, the same as for the argon plasma. The plasma potential also increased as the arc current was increased from 10 to 90 A, but in another range: from 3.3 to 4.2 V. The increase of the PINK arc current in the chosen range at a constant working gas pressure increased the plasma density in the range  $(0.2\text{--}2.0) \cdot 10^{16} \text{ m}^{-3}$ .

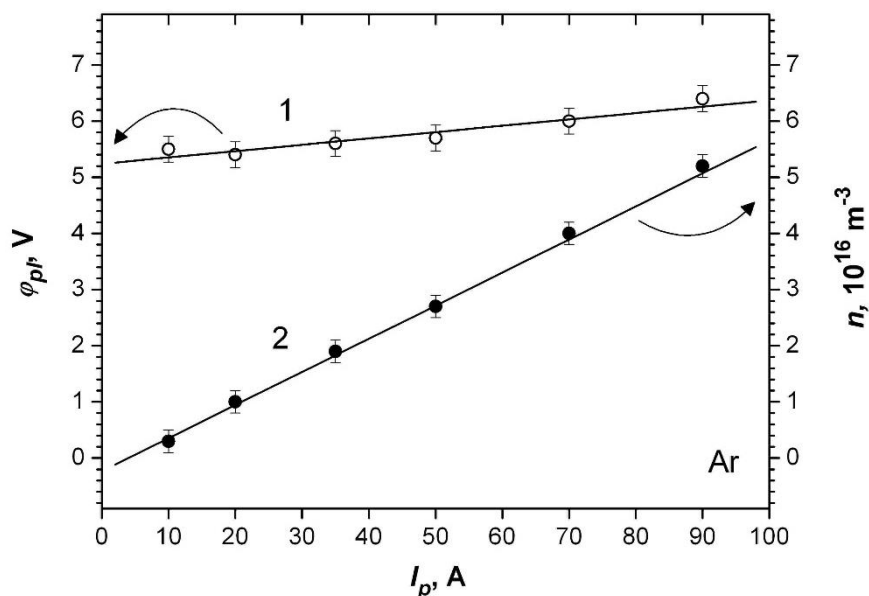


**Figure 3.** Plasma potential (curve 1) and density (curve 2) versus PINK arc current for argon plasma.

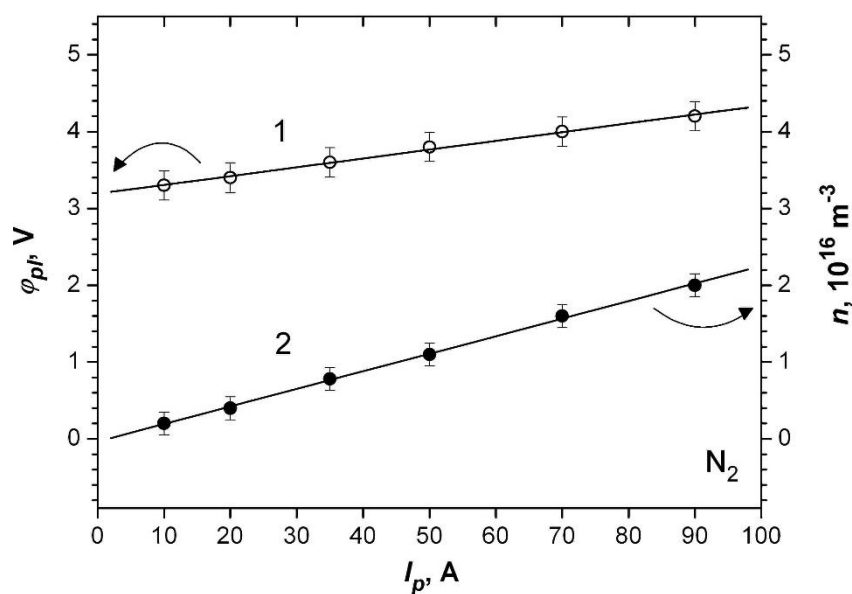


**Figure 4.** Plasma potential (curve 1) and density (curve 2) versus PINK arc current for nitrogen plasma.

### 3.2. Metal and metal-gas plasma for synthesis of coatings

The density of the metal plasma produced, not using the PINK source, with argon and nitrogen used as working gases at  $I_d = 50$  A (Fig. 5, 6) was  $2.6 \cdot 10^{16}$  and  $2.2 \cdot 10^{16} \text{ m}^{-3}$  and its potential was 3.8 and 2.4 V, respectively. The average electron temperature for the arc-generated metal (titanium) plasma was  $\sim 0.8$  eV.

When the sources of metal and gas plasmas were operated at  $I_d = 50$  A with argon used as working gas and the PINK current was increased from 10 to 50 A, the plasma potential increased from 3.8 to 5.5 V (see Fig. 5). In this case, at a fixed current of the arc evaporator, the metal-gas plasma density

increased from  $2.6 \cdot 10^{16}$  to  $4.5 \cdot 10^{16} \text{ m}^{-3}$ . When nitrogen was used as working gas, the plasma potential increased from 2.4 to 3.4 V (see Fig. 6) and the metal-gas plasma density increased from  $2.2 \cdot 10^{16}$  to  $3.0 \cdot 10^{16} \text{ m}^{-3}$ . The average electron temperature for the mixed metal-gas plasma was 0.9–1.0 eV.

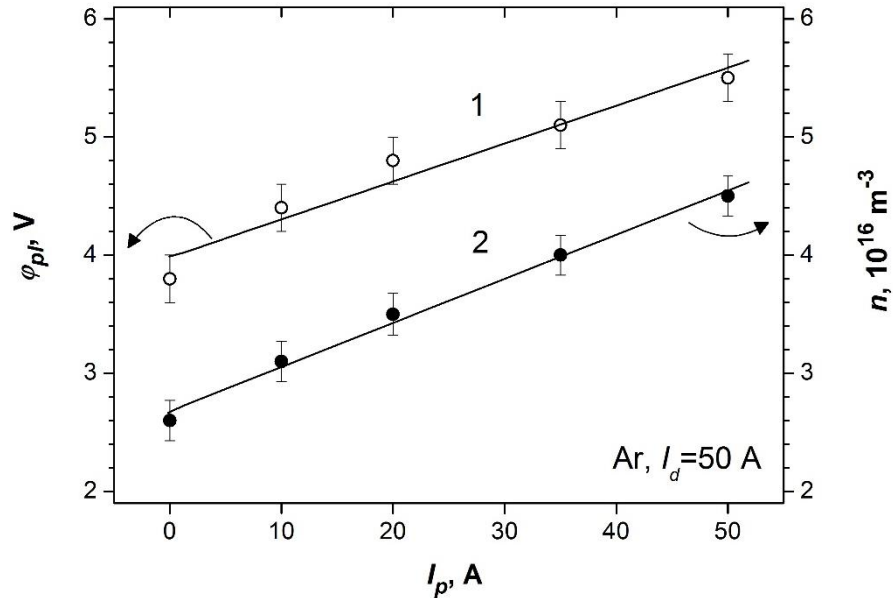


**Figure 5.** Metal-gas plasma potential (curve 1) and density (curve 2) versus PINK arc current for argon:  $I_d = 50 \text{ A}$ .

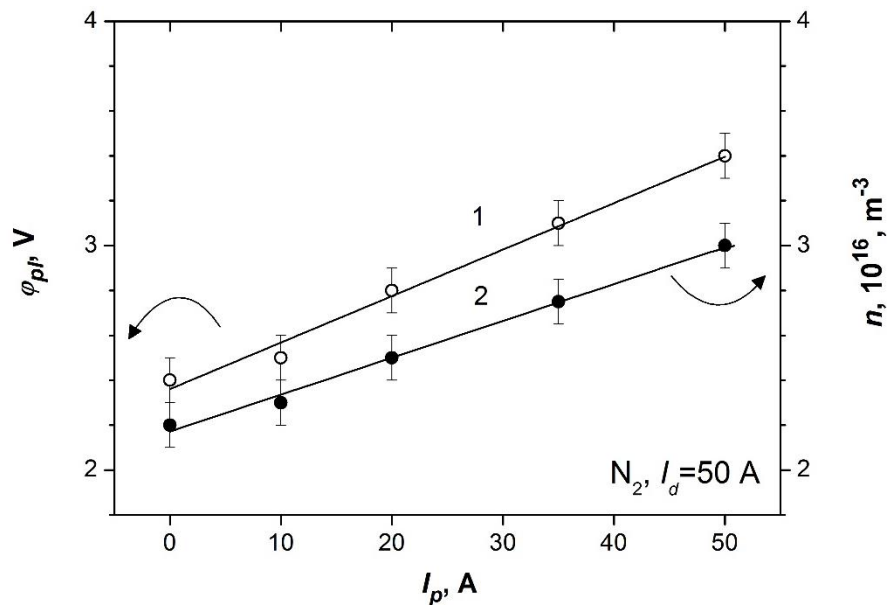


**Figure 6.** Metal-gas plasma potential (curve 1) and density (curve 2) versus PINK arc current for nitrogen:  $I_d = 50 \text{ A}$ .

It is clear that the density of the metal-gas plasma was approximately equal to the sum of the gas and metal plasma densities measured at the same arc parameters. For the doubled discharge current of the arc evaporator ( $I_d = 100 \text{ A}$ ), the plasma potential and density were also observed to vary linearly with the PINK arc current. However, in this case, the density of the mixed plasma was approximately twice that measured at a 50 A current (Fig. 7).

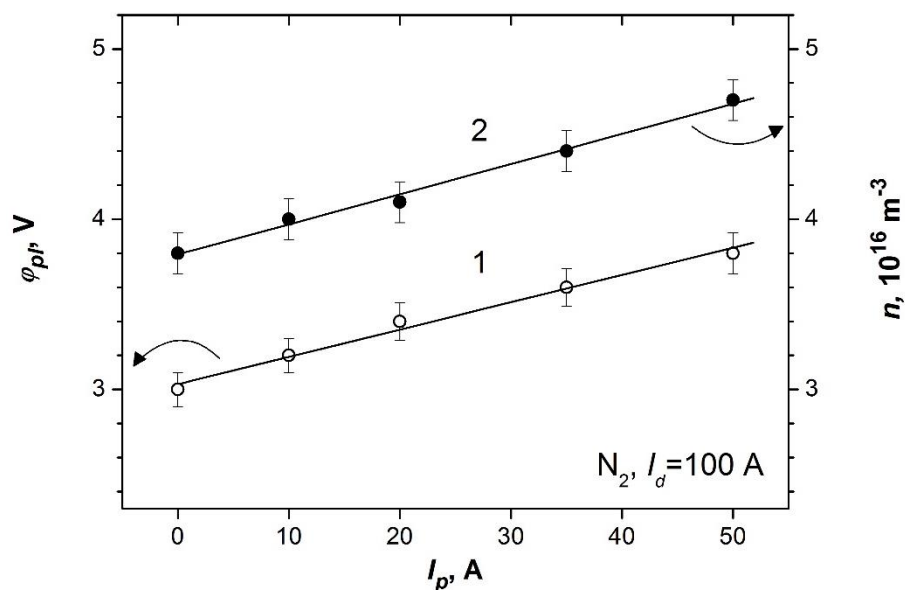


**Figure 7.** Metal-gas plasma potential (curve 1) and density (curve 2) versus PINK arc current ( $I_d = 100$  A).

### 3.3. The effect of plasma assistance on the characteristics of the coatings

The experimental data suggested that the concentration of nitrogen charged particles in plasma-ion-assisted vacuum-arc deposition of nitride coatings could be increased by increasing the PINK arc current, thus promoting the formation of nitride compounds on the substrate and in the cathode-substrate gap.

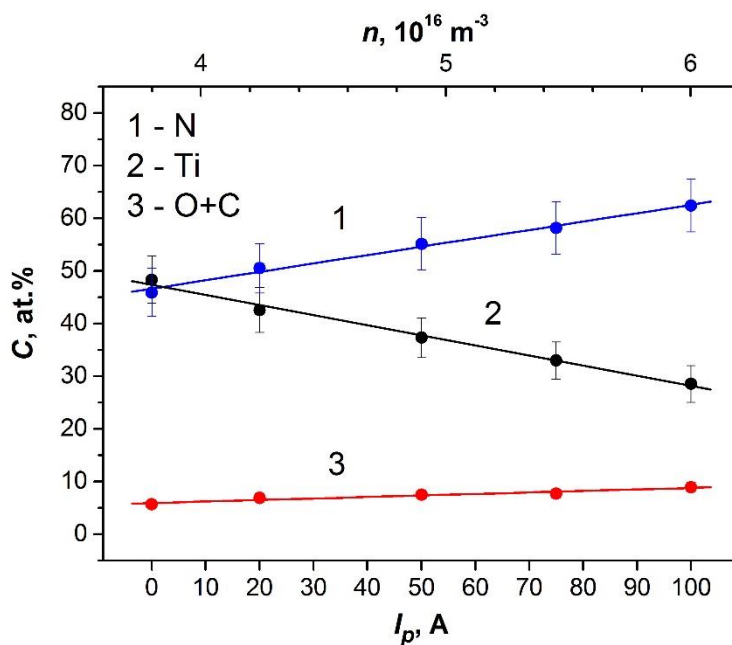


**Figure 8.** Element concentrations in TiN coatings versus PINK arc current and metal-gas plasma density.

To check this, plasma-assisted deposition of TiN coatings was performed at different PINK arc currents. The elemental composition of the coatings as a function of current is given in Fig. 8. For the TiN coatings deposited (not using the PINK source) from metal plasma in a molecular nitrogen medium at  $p_{N_2} = 0.3$  Pa, the titanium-to-nitrogen concentration ratio is, within the limits of experimental error, 1:1. The Ti:N ratio for the coating deposited with plasma assistance at a rather low PINK arc current ( $\leq 20$  A) can also be taken equal to 1:1, within the limits of experimental error. As the discharge current is further increased, and, hence, the fraction of nitrogen charged particles (gas plasma density) increases, the nitrogen content in the TiN coating increases, whereas the titanium content accordingly decreases. When the evaporator arc current and the PINK arc current are in the ratio 1:1, the concentration of titanium is approximately half that of nitrogen.

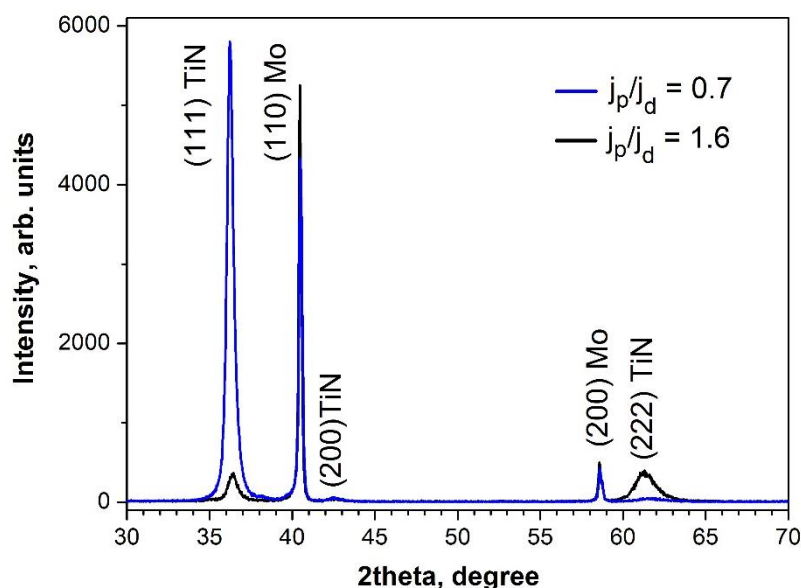


**Figure 9.** Diffraction patterns of TiN coatings deposited at different ratio  $j_p/j_d$ .

It should be noted that the color of coatings changes in dependence of increase of gas plasma source current and accordingly in dependence of nitrogen content from gold to copper-gold (Table 1). It was revealed that hardness of coatings increases from 24 GPa to 35 GPa at increasing nitrogen concentration.

**Table 1.** Parameters of TiN coatings in dependence of ratio  $j_p/j_d$ .

$j_p/j_d$	$H$ (GPa)	$CSR$ (nm)	color
0.7	24	41	gold
1.2	28	30.5	pink-gold
1.6	35	17	copper-gold



The results of X-ray analysis of TiN coatings deposited at different ratio of current densities of PINK source and arc evaporator ( $j_p/j_d$ ) are shown in Fig. 9 and Tabl. 1. It is clear, that the coating consists of polycrystalline TiN with a NaCl-type FCC structure at  $j_p/j_d=0.7$ . TiN crystallites have preferred orientation along the plane [111]. In the case the size coherent-scattering region (CSR) is 41 nm. At increase of ratio  $j_p/j_d$  up to 1.6 the considerable increasing (222)TiN reflex intensity and broadening of TiN peaks are observed. The fact deals with decreasing crystallite size as size of CSR decreased to 17 nm.

It should be noted that in all coatings synthesized by the chosen method, oxygen and carbon were detected, which was related to the conditions of evacuation. The total concentration of these elements in the coatings was not above 9 at. %. However, the authors of [19] showed that the presence of a large amount of oxygen (up to 7 at. %) and carbon (up to 4.7 at. %) in the coatings based on TiN causes no superhardness degradation. In addition, the oxygen existence in the TiN coating can be the cause of titanium oxides formation on a coating surface. It was investigated in detail by XPS analysis and shown in [20]. It should be noted that in the present work the oxide or carbide phases were not detected by X-ray analysis.

#### 4. Conclusion

The paper presents the results of an experiment performed to examine gas, metal, and mixed metal-gas plasmas. The plasmas were generated by an arc evaporator operating based on a self-sustained arc with cathode spot and by the PINK plasma source with hot filament and hollow cathode operating based on a non-self-sustained arc. The plasma sources were used independently or simultaneously, depending on the type of desired plasma. The plasma parameters were measured using a cylindrical Langmuir probe and a unique automated probe system described in the paper.

It has been demonstrated that the elemental composition of the titanium nitride coatings produced by plasma-assisted vacuum-arc deposition can be controlled by varying the arc parameters of the PINK hot filament, hollow cathode plasma source. It has been found that the PINK arc current affects the parameters of the metal-gas plasma and the element concentrations, structure and characteristics of the coatings. The effect revealed can be harnessed to synthesize 1) graded coatings where the stoichiometry could be varied varying the arc current of gas-plasma source; 2) the coatings with fine grained structure and improved mechanical properties. This could be a matter of convenience in the coating deposition using automated technological facilities.

#### Acknowledgments

The work was supported by the grant of Russian Science Foundation (Projects No 14-29-00091).

#### References

- [1] Boxman R L *et al* 1995 *Handbook of Vacuum Arc Science and Technology* (Noyes Publishing, Ridge Park NJ)
- [2] Shanyong Zhang 1993 *Journal of Materials Processing Technology* **39** 165
- [3] Saoula N *et al* 2009 *J. Plasma Fusion Res. SERIES* **8** 140
- [4] Roquiny Ph *et al* 1999 *Surf. Coat. Technol.* **116–119** 278
- [5] Sundgren J E *et al* 1986 *J. Vac. Sci. Technol. A* **4** 5 2259
- [6] Lousa A *et al* 2007 *Vacuum* **81** 1507
- [7] Wei Yongqiang *et al* 2013 *Vacuum* **89** 185
- [8] Borisov D P *et al* 1998 *IEEE Trans Plasma Sci* **26** 1680
- [9] Ryabchikov A I *et al* 2005 *Vacuum* **78** 445
- [10] Ryabchikov A I *et al* 1992 *Review of Scientific Instruments* **63** 2428
- [11] Akhmadeev Yu H *et al* 2003 *Laser and Particle Beams* **21** (2) 249

- [12] Vintizenko L G *et al* 2001 *Russ. Phys. J.* **44** 927
- [13] Koval N N *et al* 2015 *Russian Journal of General Chemistry* **85** (5) 1326
- [14] Goncharenko I M *et al* 2003 *Surf. Coat. Technol.* **169–170** 419
- [15] Ivanov Yu F *et al* 2012 *Surf. Coat. Technol.* **207** 430
- [16] Koval N N *et al* 2012 *Proceedings of the 25th International Symposium on Discharges and Electrical Insulation in Vacuum* (Tomsk, Russia) **2** 537
- [17] Koval N N *et al* 2000 *Proceedings of the 19th International Symposium on Discharges and Electrical Insulation in Vacuum* (Tomsk, Russia) **2** 590
- [18] Vershinin D S *et al* 2001 *Proceedings of the Fifth Russian-Korean International Symposium on Science and Technology KORUS '01* **1** 328
- [19] Korotaev A D *et al* 2007 *Physical mesomechanics* **10** (3-4) 156
- [20] Iordanova I *et al* 2007 *Vacuum* **81** 830